

A Parametric Study of Interface Characteristics in a Buttress Retaining Wall

Qiang-Xie

*Faculty of Civil Engineering, Chongqing University, Chongqing, China, 40004
Centro de Geotecnia, Instituto Superior Tecnico Universidade Técnica de Lisboa, Lisbon, Portugal, 1049-001; e-mail: xieqiang2000@hotmail.com*

Carlos Dinis da Gama

*Centro de Geotecnia, Instituto Superior Tecnico Universidade Técnica de Lisboa, Lisbon, Portugal, 1049-001
e-mail: dgama@ist.utl.pt*

Xianbin-Yu

*Kunming University of Science and Technology, Kunming, China, 650093
e-mail: yuxianbin@yahoo.com*

Yuxin-Chen

*Centro de Geotecnia, Instituto Superior Tecnico Universidade Técnica de Lisboa, Lisbon, Portugal, 1049-001
e-mail: cyxcfz@yahoo.com*

ABSTRACT

A parametric study was carried out to investigate the collapse of a buttress retaining wall that occurred at Malveira, Portugal. Typical values of interface properties for retaining wall problems are discussed, as well as the influence of friction, cohesion, normal and shear stiffness at the interface between the wall and soil. Results show that for this interface, the greater the friction angle is, the more the retaining wall inclines, and so does the cohesion along the interface. However, the influence of cohesion on the deformation of soil behind the wall is greater and more sensitive than that of the friction angle. The normal and shear stiffness also have significant effects upon the analysis results. A definite cause of instability happens when shear stiffness is low to maintain continuity of displacements between the wall and the retained soil. Reasonable values of stiffness are dependent on the properties of both the soil and the retaining wall. Main findings of this study are related to the advantages of using interface elements for accurately simulate the real behavior of buttress retaining walls, which indicate that the main cause of the observed collapse was due to a difference in depth with respect to the design documents, and no field measures were taken to improve the safety factor against overturning.

KEYWORDS: buttress retaining wall; collapse; parametric study; interface elements

INTRODUCTION

The subject of this research is based on buttress retaining wall collapse happened at Malveira village near Lisbon, Portugal. The scope of the work includes the determination of input parameter values, selection of appropriate calculation methods, a parametric study of interface friction between concrete wall and soil, for the calculation, development of numerical models and evaluation of results.

The most sensitive aspect on this kind of geotechnical problem is the contact simulation between concrete wall and the geological material. In early stages, the contact between different materials was supposed to be rigid, meaning that there is no interface between them and the elements in contact not allowed to slip and penetrate each other. Recently, numerical models such as FLAC3D provide an element type named "interface" which is characterized by both Coulomb sliding and/or tensile separation and thus representing more realistically interface conditions between retaining walls and geological materials.

FLAC is based upon a Lagrangian scheme which is well suited for large deflections and has been used primarily for analysis and design in mine engineering, slope stability problems and underground construction. The explicit time-marching solution of the full equations of motion, including inertial terms, permits the analysis of progressive failure and collapse^{1,2}.

BACKGROUND

The buttress retaining wall was finished in December, 2002 and Fig. 1 shows its geometry. The width of the rib is 0.3m and the distance between ribs is 4.0m.

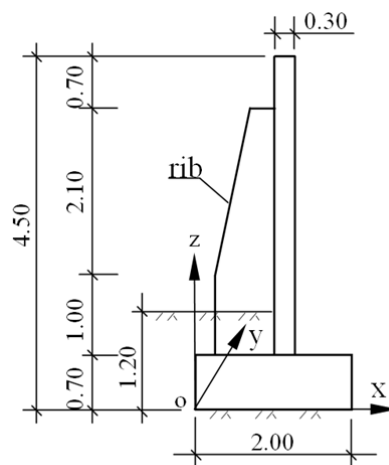


Figure 1: Dimensions of the buttress retaining wall (meters) and the placement of XYZ coordinates

THE NUMERICAL MODEL

Grid Geometry and Boundary Conditions

The FLAC model was developed on the basis of existing documents and field observations. A brick grid of 9942 zones was used for the study, comprising 446 zones for the buttress retaining wall and 9496 zones for soil. The grid is illustrated in Fig. 2 and 3.

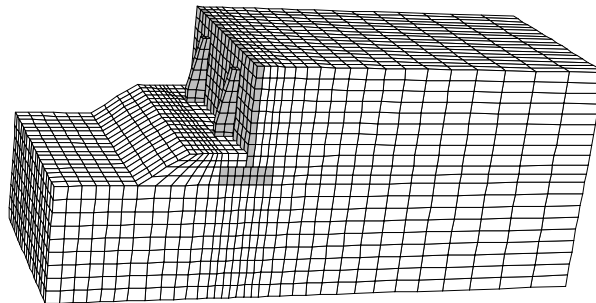


Figure 2: FLAC grid of the numerical model

A distance about 4 times of the total height of the slope was considered between the edge of the retaining wall and the right boundary of the problem, and about 2 times of the total height of the slope between the edge of the retaining wall and its left boundary.

Displacement boundary conditions were used, constraining the grid in the x-direction only at the left and right planes of the model, in the y-direction just at the front and behind planes, and in the z-direction only at the bottom boundary.

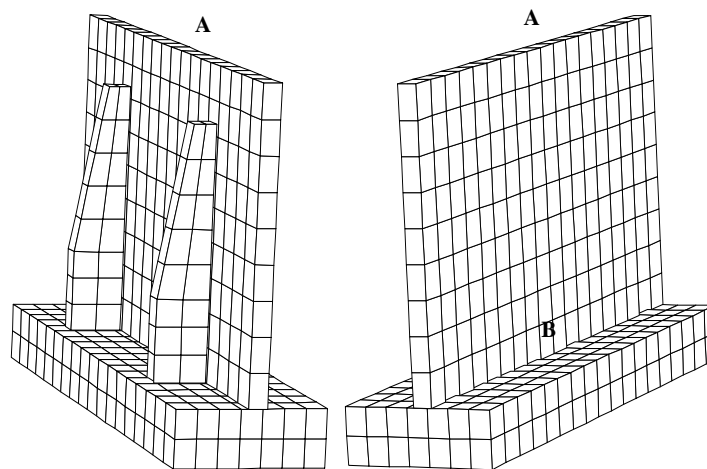


Figure 3: FLAC grid of the retaining wall

Constitutive Model and Material Properties

The Mohr-Coulomb constitutive model was selected for the soil, as it is reasonably representative of a range soil types and is very commonly used. The elastic constitutive model was selected for the concrete retaining wall because in most cases the concrete always remains in the stage of elasticity.

The acceleration gravity of 9.8 m/s^2 was applied on the model3-10.

The soil and concrete parameters are summarized in Table 1, according to the geotechnical engineering reconnaissance report.

Constant values for all parameters were initially used, except for the parameters of the interface between concrete wall and soil, because the determination of input values of interface is complex, because it is influenced by many factors such as moisture content and particle size of the soil, smoothness of the concrete wall, geometry of the retaining structure. A parametric study of interface parameters will be discussed in the following sections.

Table 1: Properties of the retaining wall materials

Property	Soil	Concrete wall
Density (kg/m^3)	2.10×10^3	2.50×10^3
Young's modulus (Pa)	5.00×10^7	3.00×10^{10}
Friction ϕ (°)	30	/
Cohesion (Pa)	1.00×10^4	/
Tensile strength (Pa)	0	2.10×10^6
Poisson's ratio	0.25	0.167

Interface Properties

Slip and separation between the retaining wall and soil are allowed which correspond to the real observed conditions.

In FLAC3D, the interface element is characterized by Coulomb sliding and/or tensile separation. Parameters include friction, cohesion, dilation, tensile strength, normal and shear stiffness values, (K_n and K_s) and should be assigned to the interface elements. Particularly K_n and K_s must be specified in all cases. In the following basic analysis, the values were set $K_n = K_s = 2 \times 10^8 \text{ Pa/m}$, as the soil equivalent stiffness. A further discussion about the influence of stiffness values on the retaining wall will be presented in Section 5.4.

From the design documents and geotechnical engineering reconnaissance report, cohesion value, dilation angle, and tensile strength were set to zero, and friction to 26.6° , corresponding to a frictional coefficient, $C_0 = 0.5$.

BASIC ANALYSIS

The results obtained upon various simulations using the interface properties are typical of this kind of analysis. In this case, the calculations converged, meaning that the slope retaining by the concrete buttress wall was stable.

Slope Deformation

Fig. 4 shows the X-direction displacement vector diagram on the section where $y = 4\text{m}$. The point with maximum displacement is located near the top of the wall under the lateral soil pressure, while the foundation is almost fixed because of the reaction of its own gravity and soil pressure in front of the wall toe. In most numerical analysis the friction between soil and concrete wall is usually ignored by researchers. They assume the interface is in a state of rigid contact or assume that there is no friction on the interface, that is to say, $C=0$ and $\phi = 0$, so that elements on both sides of the interface slip smoothly. However both assumptions do not coincide with the actual conditions. In the analysis herein, because the interface is considered in the model, relative movements occur between soil and the wall, as shown in Fig. 5. Fig. 5 shows the displacement behavior of the wall and soil on XZ plane along the path AB (Fig. 3) at the section where $y = 4\text{m}$. Deformation on each side of the interface is different because of interface elements property setting and the different characteristics of concrete wall and soil.

The wall has higher rigidity and density than that of soil, thus its displacement changes linearly with the height of the wall, while the displacement of soil reflects a certain irregular behavior. There is a turning point at 3.66m high of the wall in the soil displacement curve. It is figured out that the existence of the nearby rib has caused that. Such kind of phenomenon is easier to observe in Fig. 6.

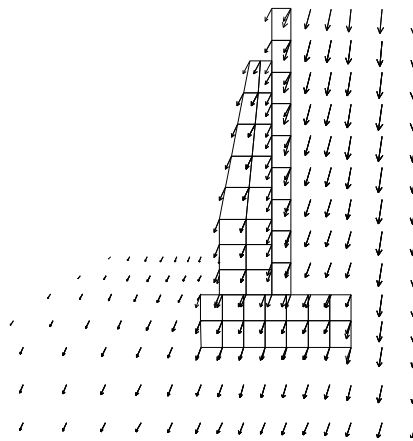


Figure 4: Displacement vectors in XZ-plane on the section where $y = 4\text{m}$

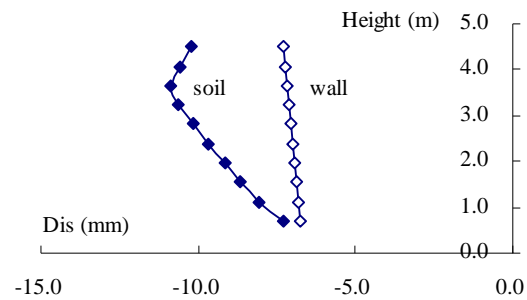


Figure 5: Displacements of the wall and the soil in XZ plane along the path AB

The straight line stands for active earth pressure curve by Rankine's theory in Fig. 6, the irregular one is the re-distribution of earth pressure curve behind the wall. The turning points lie on the location where rib size changes ($z=1.7\text{m}$) and almost the highest point of the rib ($z=3.66\text{m}$). The design of the rib has sufficiently optimized the supporting structure.

Stress Distribution and Shear Displacement on the Interface

Fig.7 shows the distribution of shear and normal stresses of the interface behind the wall, indicating that the distribution of normal stress is consistent with the lateral soil pressure in Fig. 6 and the distribution of shear stress corresponds to the displacement changes shown in Fig. 5. At the rib location, not only the shear stress but also the normal stress show a little difference with those in other zones. The buttress retaining wall ameliorates the distribution of the lateral earth pressure and the interface causes a dislocation between wall and soil.

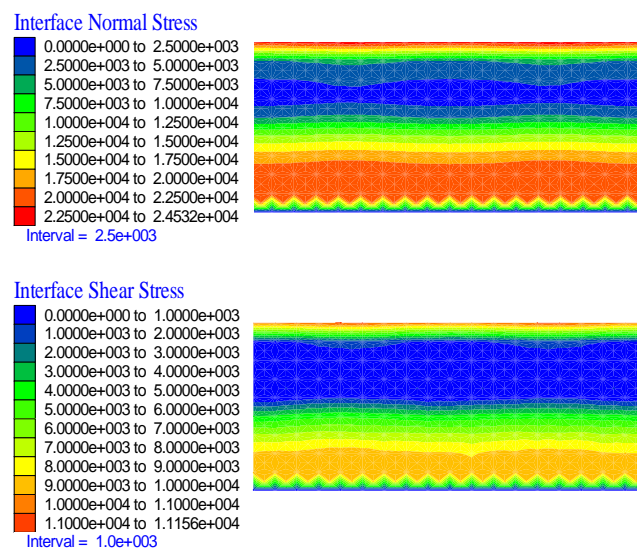


Figure 7: The shear and normal stressed at the interface behind wall

Fig.8 shows the shear and normal stresses distributions of the interface under the wall foundation.

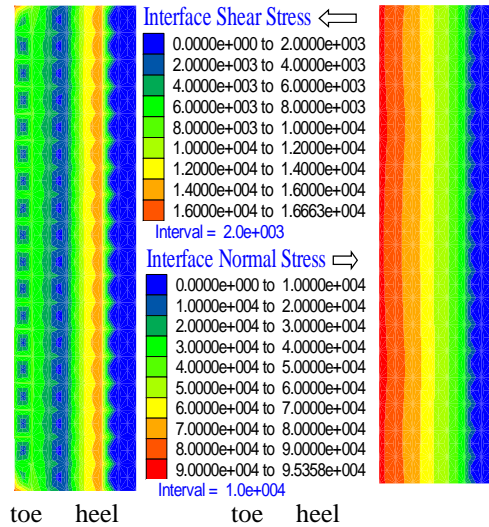


Figure 8: The shear and normal stressed at the interface under the wall foundation

The normal stress is not distributed uniformly on the wall basis because it increases progressively from its heel to the toe, mainly because of the earth pressure existence which causes the inclination of the wall over its toe, thus making the heel of the wall to separate from soil, (There, the soil is in a state of tension) but near the toe it has a tendency to be compressed. The interface shear stresses correspond to the horizontal displacement of soil, but this is not like the behavior of the interface normal stress. From the heel to the toe, the interface shear stress reflects a phenomenon of corrugation. It proves again that the wall does not move smoothly on the soil, so the friction between wall and soil is still working.

PARAMETRIC STUDY OF INTERFACE

The effects of interface properties on a retaining wall analysis can be assessed in many ways. However, in this paper, it is not possible to cover all aspects of the parametric study results. It was decided to focus on the results of greatest significance for engineering design. Thus, the parameters examined are the maximum displacement of both wall and soil behind the wall, and wall inclination.

For almost all simulations carried out, the form of results was similar. The basic shapes of the displacements of the wall and soil did not change significantly; rather it was the magnitude of the results which varied. Thus the curves shown in Fig. 4 to Fig. 8 are representative of the results as a whole. The only exceptions were some of the more extreme cases analyzed, where, for example, collapse of the soil behind the wall occurred.

Influence of the Friction Angle at the Interface Surface

Table 2 lists the frictional coefficient, C_0 between the retaining wall basis and the geological materials.

Table 2: Properties of the materials

Foundation soil		Frictional coefficient, C_0
Clay	Plastic	0.25~0.30
	Stiff plastic	0.30~0.35
	Stiff	0.35~0.45
Silt		0.30~0.40
Medium sand, coarse sand, gravel		0.40~0.50
Soil aggregate		0.40~0.60
Soft rock		0.40~0.60
Hard rock with coarse surface		0.65~0.75

The range of values used in the study is from 0° to 45° , increasing in 5° increment. The maximum value, although greater than the ϕ value used for the study, is typical of dense sand. The values therefore encompass the range of ϕ values likely to be encountered in retaining wall analyses. In the following analysis, we set cohesion along the interface $c=0$.

Fig. 9 shows the deformation of soil behind the wall on XZ plane along the path AB. All of the curves have a turning point at 3.66m high, as the curve shows in Fig.5. Below 3.66m, most of the displacements decrease with the increase of the friction angle at the interface, and there is also a small difference near a point 2.0m high where the rib size changes. While above 3.66m of the wall, deformation of soil increases with friction angles.

Fig.10 shows the changes of the inclination angle of the wall with the friction angle of the interface surface. The greater the friction angle is, the more the retaining wall inclines. Large friction angles improves the concrete wall contact with the soil, thus increasing lateral earth pressure and resulting in a more coordinated deformation between wall and soil.

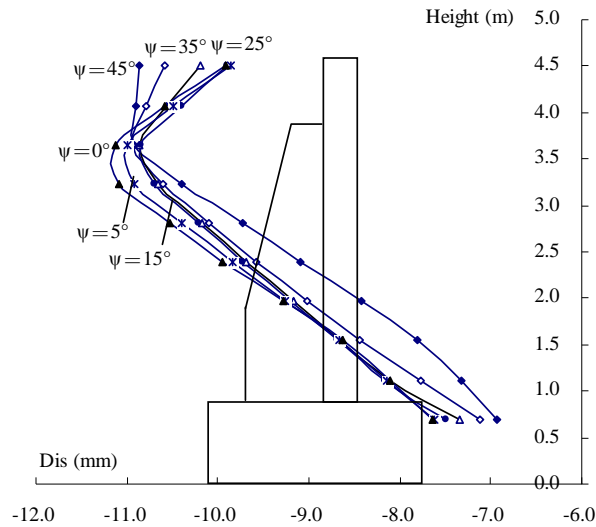


Figure 9: Displacement curves of the soil behind the wall on XZ plane along the path AB

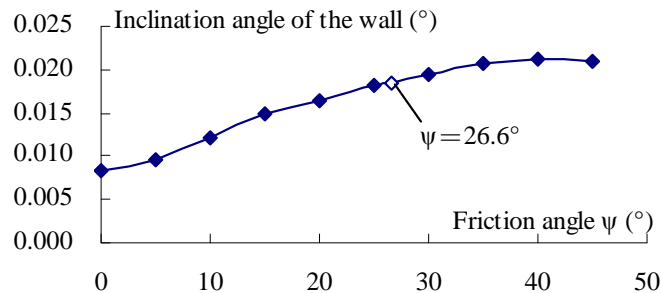


Figure 10: Changes of the inclination angle of the wall with the friction angle at the interface

Influence of Cohesion along the Interface

By Setting the frictional coefficient between the foundation of the retaining wall and the soil as a constant, to $K_0=0.5$, and cohesion along the interface used herein is 0kPa ~60kPa, increasing at 10kPa increments. The results are shown in Fig. 11.

The influence of cohesion along the interface on the deformation of soil behind the wall is greater and more sensitive than that of the friction angle. The maximum displacement of the soil behind the wall varies from about 6 to 11mm when cohesion along the interface changes from 0 to 60kPa.

The inclination angle of the wall decreases with the increase of cohesion, as shown in Fig.12. When $c=10\text{kPa}$, the inclination angle comes to a head.

Influence of the Interface Stiffness

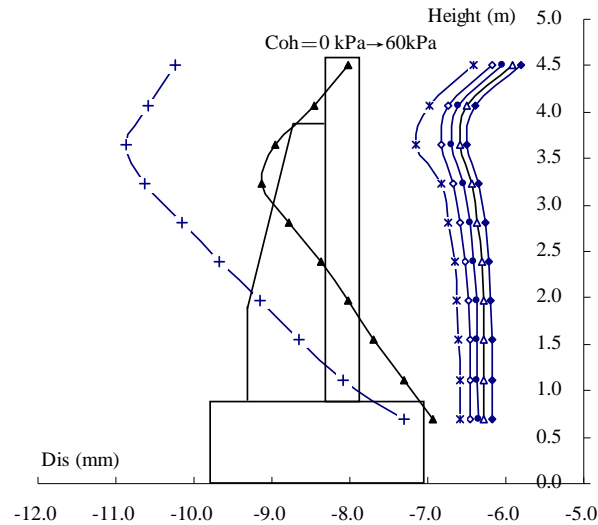


Figure 11: Displacement curves of the soil behind the wall on XZ plane along the path AB

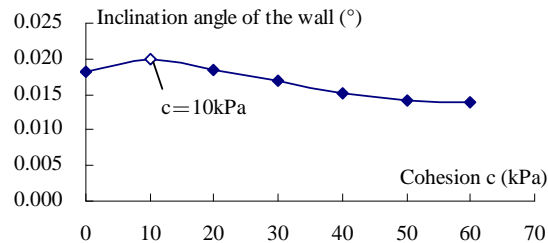


Figure 12: Changes of the inclination angle of the wall with the increase of the cohesion along the interface

Three kinds of calculations were carried out for investigating the influence of the interface stiffness values. In the following calculations, cohesion along the interface was $c=0\text{kPa}$, and the frictional coefficient, $C_0 = 0.5$.

(1) The normal stiffness is supposed to be equal to the shear stiffness, and different values of stiffness are used in the slope simulation.

Fig. 13 shows the displacement behavior of the soil behind the wall on XZ plane along the path AB (Fig. 3) at the section where $y = 4\text{m}$.

For $K_n=K_s=2 \times 10^7 \text{Pa/m}$, $2 \times 10^8 \text{Pa/m}$, $2 \times 10^9 \text{Pa/m}$, the displacement of soil behind the wall is small and changes very little. When $K_n=K_s=2 \times 10^6 \text{Pa/m}$, large deformation occurs. Till $K_n=K_s \leq 2 \times 10^5 \text{Pa/m}$, the calculation doesn't converge any more, the wall begins to collapse, as shown in Fig. 14.

(2) Setting the shear stiffness as a constant, $K_s=2 \times 10^8 \text{Pa/m}$, the range of values of the normal stiffness changes from $2 \times 10^9 \text{Pa/m}$ to 0Pa/m , decreasing 10 times for each condition. The results are shown in Fig. 15. The figure looks the same as Fig. 13. The calculation doesn't converge either when $K_n \leq 2 \times 10^5 \text{Pa/m}$. But after checking the exact position of the key points in the soil and the wall on XZ plane along path AB, it can be observed that the wall and the soil penetrate each other when $K_n < K_s$. This phenomenon does not correspond to actual conditions.

No figure is drawn here for interpreting this phenomenon, as the displacements are quite small, the contact status between wall and soil cannot be observed by naked eye.

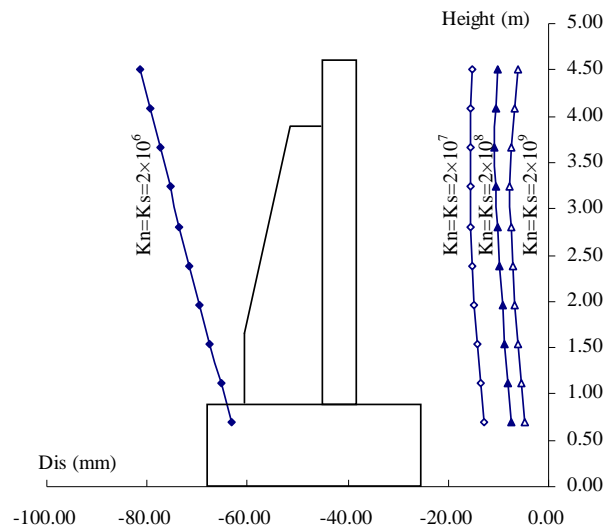


Figure 13: Displacement curves of the soil behind the wall on XZ plane along the path AB

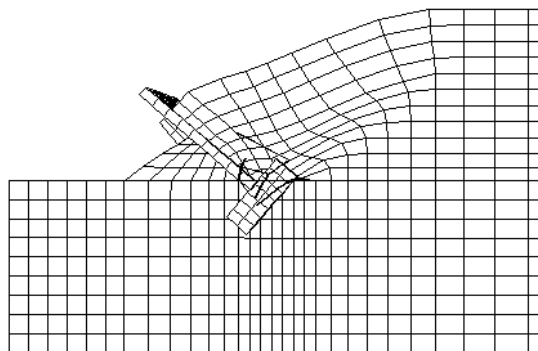


Figure 14: Wall collapses when $K_n=K_s \leq 2 \times 10^5 \text{Pa/m}$

Setting the normal stiffness as a constant, $K_n=2 \times 10^8 \text{ Pa/m}$, with the shear stiffness varies from $2 \times 10^9 \text{ Pa/m}$ to 0 Pa/m . The results are shown in Fig. 16.

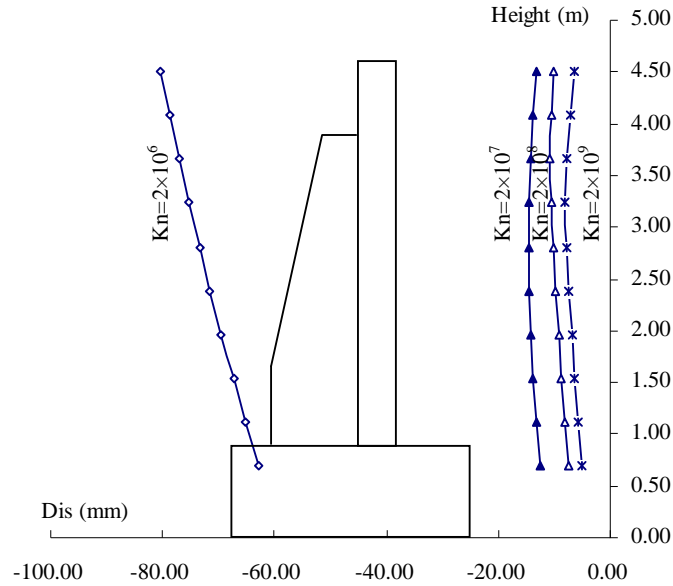


Figure 15: Displacement curves of the soil behind the wall on XZ plane along the path AB

When $K_s=2 \times 10^9 \text{ Pa/m}$ (and $K_s > K_n$), the deformation of the soil behind the wall is quite smaller than that when $K_s \leq K_n$. All calculations converge even when $K_n = 0 \text{ Pa/m}$ and no penetration occurs in all conditions. But when $K_s > K_n$, penetration occurs which does not correspond to real condition. Furthermore, when $K_s \leq K_n$, the deformation behavior of the soil behind the wall looks similar, no matter how big the difference is between K_s and K_n .

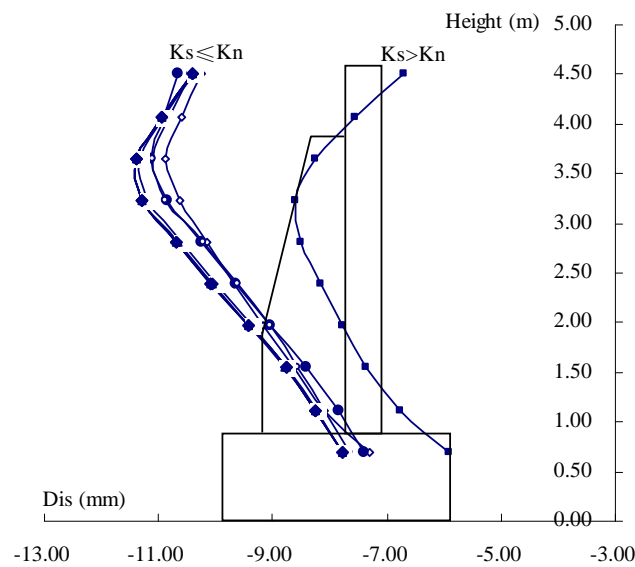


Figure 16: Displacement curves of the soil behind the wall on XZ plane along the path AB

Discussion on the Determination of Values of Interface Stiffness

The results above show that K_n should be greater than or equal to K_s . Fig. 15 and Fig. 16 indicate that if K_n and K_s are greater than or equal to the stiffness of soil, the difference of displacements of the soil behind the retaining wall is small.

In the user's manual of FLAC3D software, it is recommended that the lowest stiffness consistent with small interface deformation must be used. A good rule-of-thumb is that K_n and K_s be set to ten times the equivalent stiffness of the stiffest neighboring zone:

$$K_n = K_s = 10 \max \left[\frac{(3K + 4G)}{3Z_{\min}} \right] \quad (1)$$

where K & G are the bulk and shear moduli, respectively, and Z_{\min} is the smallest dimension of an adjoining zone in the normal direction. In this condition, $Z_{\min}=0.3\text{m}$ for both of the soil and concrete wall. So, in this case, normal and shear stiffness values, K_n and K_s of the interface equal $1.07 \times 10^{12}\text{Pa/m}$, ten times the equivalent stiffness of concrete, which is quite greater than the stiffness of soil, the value used in the above sections.

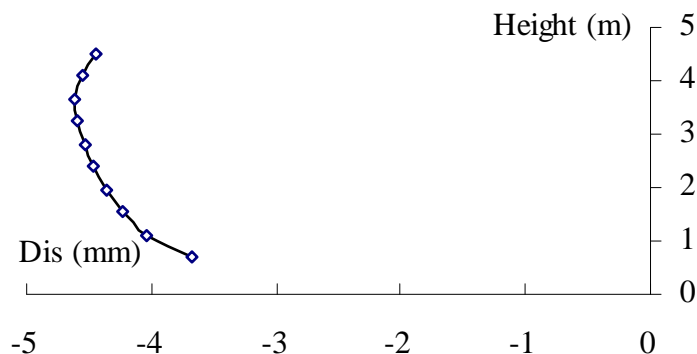


Figure 17: Displacement of the soil behind the wall on XZ plane along the path AB

Fig. 17 shows the result when $K_n=K_s=1.07 \times 10^{12}\text{Pa/m}$. The deformation behavior is the same as that when K_n and K_s are greater than or equal to the stiffness of the soil, but the maximum displacement of the top point on XZ plane is 18.6% less.

FIELD OBSERVATIONS

As demonstrated in the above calculation, if the buttress retaining wall was constructed as designed, it will be in a state of safety. But unfortunately, the actual depth of soil is 5.10 m not 4.5 m, and no more actions were taken to increase the safety factor. The embedded depth of foundation is still 1.2 m, and the widths of the wall and the ribs didn't change. According to Muni

Budhu¹¹, the recommended safety factor against overturning is 1.5, and for a 5.10 m high slope it becomes 1.10, which is quite insufficient. As obtained by FLAC 3D analysis, the wall collapses looks like that in Figure 14. Figure 18 is a photo showing the slope failure in situ.

CONCLUSIONS

The use of interface elements was adequate to allow the modeling of slip between the retaining wall and soil, which corresponds to the real field conditions. According to the FLAC3D parametric study, the following conclusions were obtained:

(1) From the basic analysis, a turning point at the 3.66m high in the soil displacement curve and the active earth pressure curve is observed. This proves that the design of the rib has sufficiently optimized the supporting structure. Furthermore, an interesting phenomenon of corrugation of interface shear stress occurs on the wall foundation, because of the friction between the wall and soil, which will not be observed if rigid links are used between different materials.



Figure 18: Collapse of the retaining wall

(2) The greater the friction angle at the interface surface is, the more the retaining wall inclines, so does the cohesion along the interface. But the influence of cohesion on the deformation of soil behind the wall is greater and more sensitive than that of the friction angle.

(3) The normal and shear stiffness values, K_n and K_s must be specified for case studies. K_n should be greater than or equal to K_s , or penetration will occur between different materials, which does not correspond to actual condition. It sounds reasonable that the values of K_n and K_s are recommended to be set to ten times the equivalent stiffness of the stiffest neighboring zone. The displacements are 18.6% bigger when K_n and K_s are set to the equivalent stiffness of the softest

neighboring zone, though the stiffness of the stiffest zone is about 500 times greater than that of the softest zone.

(4) The simulation with FLAC3D indicated that main causes of the retaining wall collapse were not only the values of parameters for slope calculation but the fact that when the real depth of soil was not the one admitted in the geotechnical engineering reconnaissance report, so that no practical measures were taken to improve the safety factor against overturning. The findings in this paper are consistent with the results from the other researchers¹²⁻²¹.

ACKNOWLEDGEMENTS

This work was financially by Land Resources and Housing Management Bureau of Chongqing (No. CQGT-KJ-2012021).

REFERENCES

1. Anna Scotto di Santolo and Aldo Evangelista (2011) "Dynamic active earth pressure on cantilever retaining walls", *Computers and Geotechnics*, 38(8): 1041-1051.
2. S. Benmebarek, T. Khelifa, N. Benmebarek (2008) "Numerical evaluation of 3D passive earth pressure coefficients for retaining wall subjected to translation", *Computers and Geotechnics*, 35(1): 47-60.
3. Cundall P.A (1993) "Explicit finite difference methods in geomechanics. Numerical Methods in Engineering". Proc of the EF Conference on Numerical Methods in Geomechanics, Blacksburg,VA", 1:132-150.
4. J. Pooley (1999) "Pile coupling spring properties for embedded retaining wall analysis". *FLAC and Numerical Modeling in Geomechanics*, Detournay & Hart (eds). Balkema, Rotterdam.
5. Chia-Cheng Fan and Yung-Show Fang (2010) "Numerical solution of active earth pressures on rigid retaining walls built near rock faces". *Computers and Geotechnics*, 37(7): 1023-1029.
6. Anne-Sophie Colas, Jean-Claude Morela (2010). "Full-scale field trials to assess dry-stone retaining wall stability". *Engineering Structures*, 32(5) : 1215-1222
7. Yuan-Jun Jiang and Ikuo Towhata (2012). "Experimental Study of Dry Granular Flow and Impact Behavior Against a Rigid Retaining Wall". *Rock Mechanics and Rock Engineering*, pp 1-17.
8. Paul F. McCombie, Chris Mundell (2012) "Drystone retaining walls: Ductile engineering structures with tensile strength". *Engineering Structures*, 45: 238-243.

9. S. Caltabiano, E. Cascone (2012) "Static and seismic limit equilibrium analysis of sliding retaining walls under different surcharge conditions". *Soil Dynamics and Earthquake Engineering*, 37: 38-55.
10. Ching-Chuan Huang and Woei-Ming Luo (2009) "Behavior of soil retaining walls on deformable foundations". *Engineering Geology*, 105(1): 1-10.
11. Muni Budha (2000) *Soil Mechanics and Foundations*, John Wiley & Sons, Inc.
12. S. Benmebarek, T. Khelifa (2008) "Numerical evaluation of 3D passive earth pressure coefficients for retaining wall subjected to translation". *Computers and Geotechnics*, 35(1): 47-60.
13. PENG Shu-quan, LI Xi-bing, FAN Ling (2012) "A general method to calculate passive earth pressure on rigid retaining wall for all displacement modes". *Transactions of Nonferrous Metals Society of China*, 22(6): 1526-1532.
14. Víctor Yepes, Julian Alcala (2008) "A parametric study of optimum earth-retaining walls by simulated annealing". *Engineering Structures*, 30(3): 821-830.
15. Ali Ghanbari and Mahyar Taheri (2012) "An analytical method for calculating active earth pressure in reinforced retaining walls subject to a line surcharge". *Geotextiles and Geomembranes*, 34: 1-10.
16. F. Askari, A. Totonchi (2012) "Application of admissible stress fields for computation of passive seismic force in retaining walls". *Scientia Iranica*, 19(4): 967-973.
17. Ł. Widuliński, J. Tejchman (2011) Discrete simulations of shear zone patterning in sand in earth pressure problems of a retaining wall. *International Journal of Solids and Structures*, 48(7): 1191-1209.
18. Tufan Cakir (2013) "Evaluation of the effect of earthquake frequency content on seismic behavior of cantilever retaining wall including soil-structure interaction". *Soil Dynamics and Earthquake Engineering*, 45: 96-111.
19. Anna Scotto di Santolo, Lorenza Evangelista (2012). "Influence of Suction on the Behaviour of Retaining Walls in the City of Naples, Italy". *Unsaturated Soils: Research and Applications*, pp 275-282.
20. Sengupta (2012) "Numerical Study of a Failure of a Reinforced Earth Retaining Wall". *Geotechnical and Geological Engineering*. 30(4): 1025-1034.
21. Chungsik Yoo (2004) "Performance of a 6-year-old geosynthetic-reinforced segmental retaining wall". *Geotextiles and Geomembranes*, 22(5): 377-397.

